

Electron localization in dense helium gas: New experimental results

K. W. Schwarz

IBM Thomas J. Watson Research Center, Yorktown Heights, New York 10598

(Received 20 July 1979)

New experimental results on the transport behavior of electrons in dense helium gas at liquid-helium temperatures are presented. These include accurate measurements of the initial deviation of the mobility from the classical Boltzmann behavior as the density is increased and a complete characterization of the hot-electron behavior through the localization transition. The initial deviations at these temperatures are found to be of the same form as those observed in previous high-temperature studies, and a universal relationship is proposed. Contrary to an assumption that has often been made, there appears to be no reason to consider the initial deviation and the localization transition as distinct phenomena. A comparison with the percolation model of Eggarter and Cohen yields surprisingly good agreement over the whole range of densities and temperature. The role played by the helium-gas problem in the field of disordered materials is discussed, and possibilities for further theoretical progress are pointed out.

I. INTRODUCTION

In the study of the electronic states of disordered systems, one of the most interesting problems is that of an electron interacting with a dilute gas of hard spheres. This system appears to represent a sufficiently simple example of a three-dimensional random medium to offer some hope of theoretical development, and it can be approximately realized in the laboratory by injecting excess electrons into helium gas. Although considerable experimental and theoretical work has been done on this unusually elegant and well-characterized prototype of a disordered system, these efforts have been somewhat episodic, and there is no clear consensus on the correct interpretation of the experimental results. Thus, ample opportunity exists for further progress.

We first sketch some of the basic features of the problem. The scattering of a low-energy electron from a noble-gas atom can be described in terms of a repulsive core of radius 0.5–0.75 Å, representing the effect of the closed shells, plus an attractive polarization potential acting only at a radius greater than 1.5–2 Å.¹ In the case of helium, the polarizability is so small that the repulsive core dominates the scattering: The interaction is described by a positive scattering length $a_0 = 0.63$ Å, and the cross section does not depart significantly from $4\pi a_0^2$ for electron energies in the thermal range.² Thus, electrons in helium gas will see a random distribution of hard-sphere-like scatterers which can be thought of as stationary since their thermal velocities are very low relative to those of the electrons. Furthermore, the gas of scatterers is dilute in the sense that $na_0^3 \ll 1$ for all densities n of interest.

Experimental studies have so far confined them-

selves to measuring the steady-state drift velocity v_D of the electrons in a constant electric field E , under various conditions of gas temperature and density. Early work was done at low densities and high temperatures, where the classical Boltzmann equation is applicable. In this regime, v_D is a universal function $v_D(E/n, T)$, the exact form of which depends on how the momentum transfer cross section σ varies with energy.³ In fact, measurements of this function are used to determine $\sigma(\epsilon)$.² At low fields the usual linear dependence $v_D = \mu E$ obtains, and the classical mobility μ_{class} can be derived explicitly,

$$\mu_{\text{class}} = \frac{4}{3} \frac{e}{(2\pi m k T)^{1/2}} \frac{1}{n \sigma_0}, \quad (1)$$

where m is the electron mass and σ_0 denotes the zero-energy limit of the cross section.⁴

Large deviations from the classical behavior have been observed at high gas densities and at low temperatures. As it happens, these studies have been carried out in two phenomenologically distinct areas of interest. In the first of these, the aim has been to extend the traditional measurements to very high densities in order to test the limits of the classical description.^{5,6} Figure 1 shows that an anomalous decrease in μ is observed, approximately linear in n and becoming more pronounced at lower temperatures. Similar behavior has been seen for other scatterers,^{7,8} e.g., H_2 and N_2 , which also exhibit a positive scattering length for electrons. A second group of investigations⁹⁻¹¹ is connected with the fact that in liquid helium, or in the dense gas at helium temperatures, electrons exist only in self-trapped bubble states where the electron wave function is confined to a small spherical region from which the helium is excluded. Figure 2 shows that, as n is

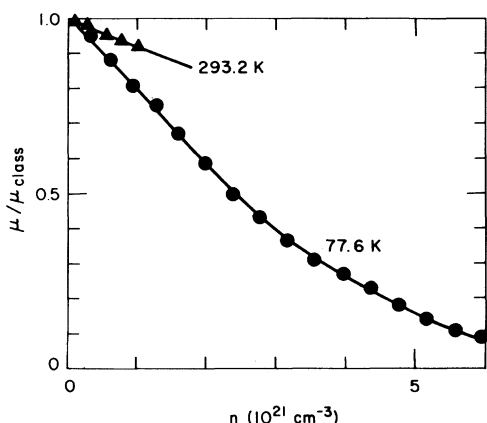


FIG. 1. Ratio of the actual mobility of electrons in helium gas to that calculated from the classical result of Eq. (1) (after Refs. 5 and 6).

increased at these temperatures, the mobility drops several orders of magnitude from the classical value to the very low values characteristic of electron bubbles. Measurements of this type have therefore been carried out with the idea of studying the transition between the free-electron regime and the self-trapped regime.

Despite the fact that both groups of measurements deal with essentially the same phenomenon, there has been relatively little overlap: The high-temperature results have not been extended to sufficiently high densities to observe the low mobilities characteristic of the bubble state, and the

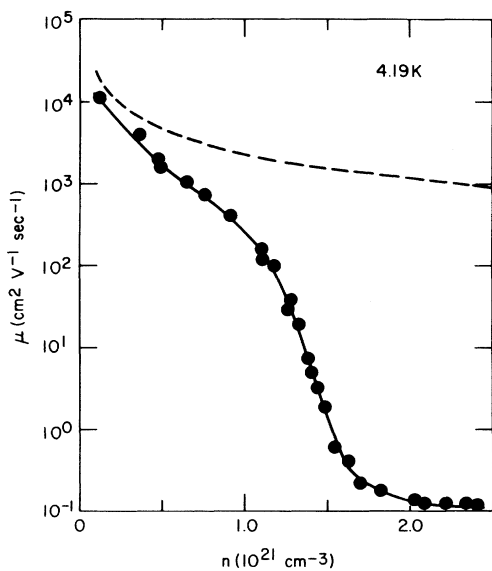


FIG. 2. Mobility at 4.19 K (after Ref. 9). The dashed line shows the prediction of Eq. (1).

low-temperature measurements have not been sufficiently accurate at the lower densities to permit comparison with the high-temperature data. A similar division exists in the way the results have been approached theoretically: Analysis of the high-temperature data has aimed at patching up the classical theory of free-electron transport; analysis of the low-temperature data has concentrated on the transition of the electrons to the bubble state, with the implicit assumption that this process is similar to a first-order phase transition. Several authors, however, have taken the more sophisticated approach of treating the gas as the source of a random potential acting on the electron, and applying the ideas which arise in the theory of disordered systems. This approach will be discussed in the next few paragraphs.

Even in the high-temperature experiments the thermal wavelength of the electrons is usually larger than the interatomic distance, and it is natural to ask whether their wave nature should enter into consideration. A simple answer is that the classical Boltzmann equation is not valid unless the characteristic wavelength of the electrons is much less than their mean-free path. When this condition breaks down, the electron wave interacts simultaneously with several scattering centers and the usual complications associated with random quantum-mechanical systems begin to arise. Figure 3 shows that this occurs at readily accessible temperatures and pressures. On a slightly more sophisticated level, one can treat the multiple scattering effects as giving rise to a constant effective potential $V(n) = 2\pi\hbar^2 n a_0/m$ in which the electrons move, their mean-free path being unaffected.^{12,13} The Boltzmann formalism is then

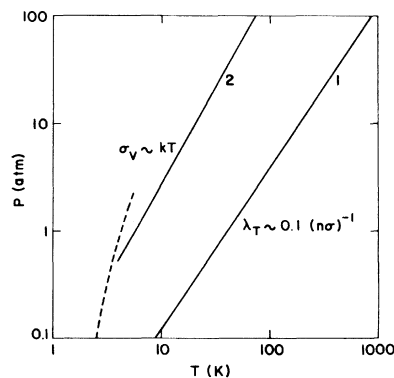


FIG. 3. Curve 1: Conditions under which the electron thermal wavelength becomes significant compared to the electron mean free path. Curve 2: Conditions under which the fluctuations in the effective potential seen by the electron become comparable to kT (after Ref. 14). The dashed line is the vapor-pressure curve.

recovered, and, indeed, higher-order effective medium approximations are possible in which the mean-free paths as well as the energies of the electrons are renormalized.

In addition to being formally very complicated, the effective medium approximations tend to run into trouble for electron energies near $V(n)$, where the kinetic energy becomes small. The reason for this can be appreciated on the basis of the following argument.¹⁴ Let us suppose that the effective potential seen by the electron at a point \vec{r} is $\bar{V}(\vec{r}) = V[n(\vec{r})]$, where $n(\vec{r})$ is a local density determined by counting the number of scatterers contained within some characteristic averaging volume L^3 . Since L^3 is finite, $n(\vec{r})$ and consequently $\bar{V}(\vec{r})$ will be fluctuating quantities. It is easy to show that, for an ideal gas and a large enough L , $n(\vec{r})$ has a Gaussian distribution with a standard deviation $\sigma_n = (n/L^3)^{1/2}$. How L should be defined is a matter of some conjecture, but one possibility¹⁴ is to take it to be on the order of the free-space wavelength $h/(2m\epsilon)^{1/2}$ of the electron. Now if the kinetic energy of the electrons is much greater than the variation $\sigma_V = \sigma_n(\partial V/\partial n)$ in \bar{V} , it is possible to use an effective medium picture and ignore the fluctuations. At sufficiently low energies, however, the electrons will be strongly affected by the fluctuations, and will eventually become localized in regions of minimum \bar{V} . This regime raises the difficult questions characteristically associated with the theory of localization in disordered systems. Conversely, it provides an opportunity to study them experimentally. The fluctuation-dominated regime can be attained either by lowering the electron energy (i.e., the temperature) or by increasing σ_V (i.e., the gas density). Figure 3 shows the pressure and temperature at which $\sigma_V = kT$, if L is assumed to have the value given above. One may conclude that the fluctuation-dominated regime should also be easily accessible in the helium-gas system.

A comparison of Figs. 1–3 indicates that such arguments, in which the gas is treated as a random medium, may indeed suffice to explain the observed behavior. To go beyond this general supposition, however, it is necessary to develop a specific theoretical model, presumably based on some of the approximations popular in the theory of disordered systems, and to compare its predictions with measurements of the electron drift velocity as a function of electric field, gas density, and temperature. As has been pointed out above, neither the theoretical nor the experimental parts of this enterprise have been carried to the point where a coherent picture has emerged. We have therefore performed an experiment to obtain additional information. Particular empha-

sis has been placed on establishing the connection between the two groups of measurements represented by Figs. 1 and 2. Extensive data on the hot-electron behavior at low temperatures are also presented. The results are compared to previous measurements and an overall picture of the experimental situation is given. The theoretical aspects of the paper are limited to a brief discussion of the extent to which extant theoretical models are relevant to this overall picture. A preliminary report on the work presented here has been published previously.¹⁵

II. EXPERIMENTAL PROCEDURES

As in previous experiments, excess electrons are injected into ^4He gas and their equilibrium drift velocity v_D is measured as a function of the applied electric field E , the gas number density n , and the temperature T . The drift velocity is determined by generating a low-density pulse of electrons, letting it drift through the gas under the influence of a uniform field, and observing its arrival at a collector C by means of a fast electrometer.¹⁶ Typical signal-averaged response curves are shown in Ref. 16.

The measurements were carried out using two different electrode configurations, the more frequently used of which is indicated in Fig. 4. Gas in the region R - S is ionized by α activity plated as shown. The repeller R and the drift region S - G are biased so as to provide a steady electron current, which is then gated by applying relatively small voltages between the wires of a parallel-wire chopper grid CH . The effective drift space here is the region CH - G , which for these measurements had a length of 1.85 cm. In the other measurement configuration, the chopper grid was removed and a grid was placed across the opening in S . Negative voltages applied to the repeller then inject electron pulses into the drift space S - G , which is 3.70 cm in length. Drift velocities obtained by means of these two arrangements agreed

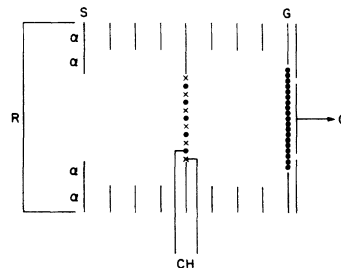


FIG. 4. Primary electrode configuration used in determining drift velocities. See the text for discussion.

to within 2%. In either method the measured drift velocities did not depend on the voltages in the source and collector regions, or on the size of the gating pulses, or on which edge of the pulse was used to determine the flight time.

The electrode assembly is contained in a thick-walled copper can immersed in the liquid-helium bath. Temperature is measured by an Allen-Bradley carbon resistor located inside the can, and controlled by a heater wire wound uniformly around the outside of the can, in direct thermal contact with the bath. The resistance thermometer is calibrated by filling the can with just enough liquid to cover the resistor, and measuring its vapor pressure.

The temperature range studied was 2.7 to 5.0 K. In this range, the helium bath can support very large temperature gradients. In practice, these are minimized by always pumping down to the working temperature, thus causing convective mixing in the bath. With the additional temperature equalization provided by the copper walls of the can, there seemed to be no difficulty in establishing a uniform temperature in the gas inside the can. The absolute uncertainty in T , arising from the combined effects of residual temperature gradients and of errors in the calibration points, is estimated to be of order ± 0.01 K at worst.

^4He gas from an ordinary cylinder was admitted to the evacuated can through a nitrogen-cooled charcoal trap. Upon occasion, the can was filled with very pure gas obtained from storage-Dewar boil-off. At other times, air impurities were deliberately added. While a large dose of impurities had the temporary effect of reducing the signal current, these were soon frozen out, and no evidence was found to indicate that impurities were affecting the measured drift velocities.

The pressure of the gas was determined by means of a calibrated quartz Bourdon tube gauge. Over most of the range of interest the gas density was then calculated from the virial equation, using the virial coefficients determined by Kilpatrick *et al.*¹⁷ from the data of Keller.¹⁸ This procedure is expected to yield n with an accuracy of order 1%. In the greater vicinity of the critical point, the virial equation is not sufficient, nor does a better equation seem to be available, except very near the critical point. To deal with this difficulty, $n(P)$ isotherms were generated by interpolating between the virial equation at lower densities and the known values of n at the saturated vapor pressure.^{18,19} The interpolation was carried out by extrapolating back from the saturated vapor pressure using the critical-point equation of Verbeke,²⁰ but with the correct saturated vapor pressure substituted into his equation explicitly. This

is not a particularly satisfactory procedure, and for that small part of the data taken at high densities and temperatures near 5 K, the error in n can be as much as several percent.

Several factors limited the range of densities over which complete $v_D(E)$ curves could be obtained. At low densities the mobility becomes large, and it is necessary to use very small fields in order to explore $v_D(E)$ down into the linear region. As the field is reduced, however, the signal becomes weaker, dropping to zero at a finite, history-dependent value of E . Measurements of μ at small n therefore require careful procedures to assure that they are being made in the linear regime. It was in fact found that previously reported determinations of μ at small n were quite inaccurate and not suitable for comparison with the high-temperature results of Bartels.⁶

Measurements at the very highest velocities were limited by the response time of the electrometer and by the resolution of the digital signal averager used to acquire the data. The $1/e$ rise-time of the electrometer was about $2 \mu\text{sec}$. As explained in Ref. 16, this means that $\frac{1}{2} \mu\text{sec}$ must be subtracted from the flight times determined from the pulse edge. The signal averager had a minimum dwell time of $1 \mu\text{sec}$ per channel. Combining this with the absolute error found by comparing results obtained with the two electrode configurations, one obtains a conservative error estimate for the drift time of $\pm 2\%$ or $\pm 1 \mu\text{sec}$, whichever is larger. In general, the long-term repeatability of the results was well within these limits.

Finally, it was found that arcing problems imposed a density-dependent upper limit to the field beyond which measurements could not be made. As a consequence, it was not possible to explore the nonlinear part of the $v_D(E)$ curve at high gas densities.

An overall test of the experimental methods was made by measuring $v_D(E)$ at liquid-nitrogen temperatures. Figure 5 shows how the results compare with the very precise determination of Crompton *et al.*² Such differences as exist are well within the error estimates given above. An additional check was made by remeasuring μ in liquid helium. Values obtained with the present cell were within $\frac{1}{2}\%$ of those reported previously.¹⁶

III. RESULTS

Measurements of the low-field response, i.e., of the zero-field mobility μ , will be described first and compared with previous results. It is important to remember that in these measurements, the electrons do not interact with each

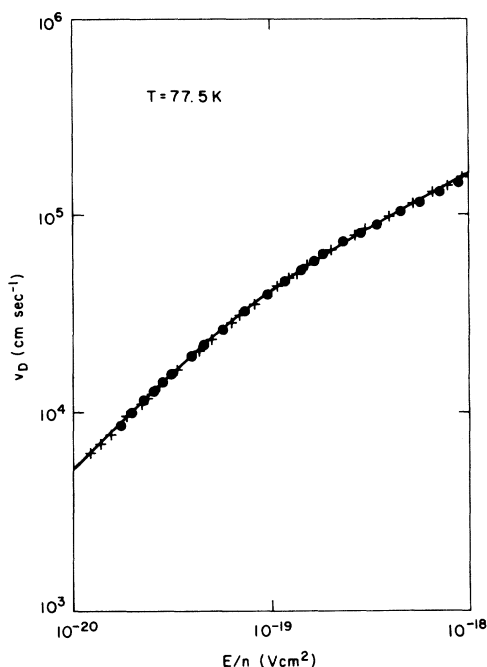


FIG. 5. Comparison of results obtained in the present experiment at 77.5 K with values derived from the precision data of Ref. 2 (solid line). The dots and crosses represent drift velocities measured at $n = 0.097 \times 10^{21}$ and 0.167×10^{21} atoms/cm³, respectively, using the electrode geometry of Fig. 4.

other, but only with the gas. Furthermore, it is found experimentally that the pulse shapes are not significantly distorted when they arrive at the collector. Hence, every electron in the pulse has had time to take a statistical average over the available density of electronic states $N(\epsilon)$, and μ represents an average property of the electron in thermal equilibrium with the gas. The hot-electron behavior, described in Sec. IIIB, represents a more complicated nonequilibrium average which, in general, will be more difficult to interpret.

A. Zero-field mobilities

Figures 6–8 show the measured values of μ . The values quoted by Levine and Sanders are too low by a factor of about 2 at the lowest densities, too high by as much as 40% in the region where μ is dropping rapidly, and correct to within 10% in the high-density limit. The values quoted by Harrison *et al.* are also much too low at the lowest densities, and are too high by about 15% at densities above $n \cong 0.9 \times 10^{21}$. Except for the large deviations as $n \rightarrow 0$, which probably arise from the presence of electron heating effects in the earlier experiments, the errors are not much greater than the experimental uncertainties quoted by these authors. The more accurate and extensive

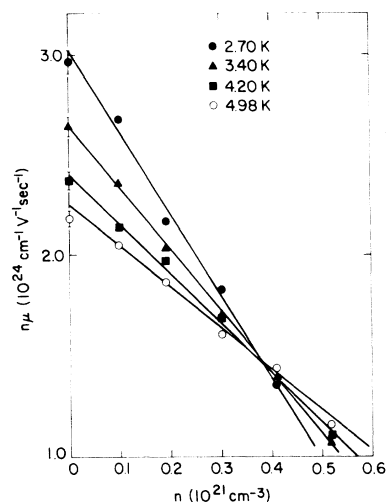


FIG. 6. Measured values of the zero-field mobility at low gas densities. The points on the $n = 0$ axis are computed from Eq. (1), using $\sigma_0 = 4.94 \times 10^{-16} \pm 2\%$ cm².

results obtained in the present experiment provide significant new information about the behavior of μ as $n \rightarrow 0$, about the temperature dependence of $\mu(n)$ in the regime below 5 K, and about the behavior of μ in the high-density limit. These will be discussed in turn.

Perhaps most interesting are the low-density results, plotted in Fig. 6. It is at once apparent that the initial linear drop-off observed previously at high temperatures (Fig. 1) is present also at helium temperatures. Figure 9 compares data ranging from room to helium temperatures, all of which show the same basic effect. Some of the

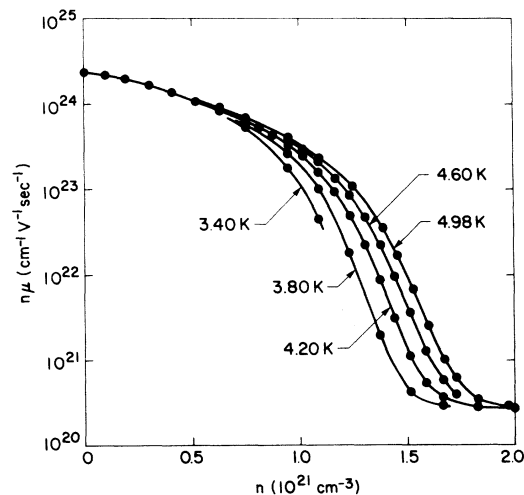


FIG. 7. Measured values of the zero-field mobility in the region of rapid drop-off. Note that the effect of small temperature differences is accurately resolved.

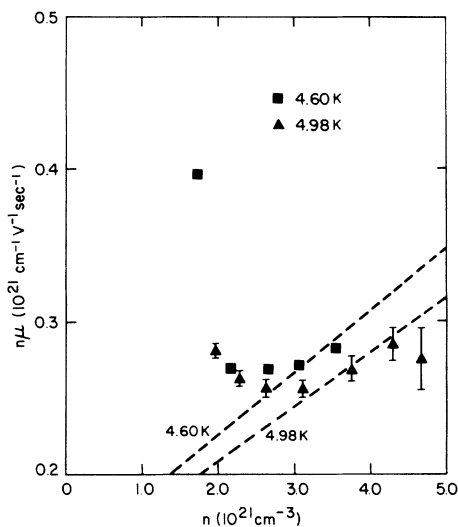


FIG. 8. Measured values of the zero-field mobility in the high-density limit. The dashed curves are derived from Eq. (4), using $R = 16 \text{ \AA}$.

data at intermediate temperatures are unreliable as $n \rightarrow 0$, and have been extrapolated to the classical limits as shown.

It is perhaps more than a mere curiosity that both the density and temperature dependence shown in Figs. 6 and 9 can be derived from a simple phenomenological argument. If one takes at face value the idea that deviations from classical behavior become important when the characteris-

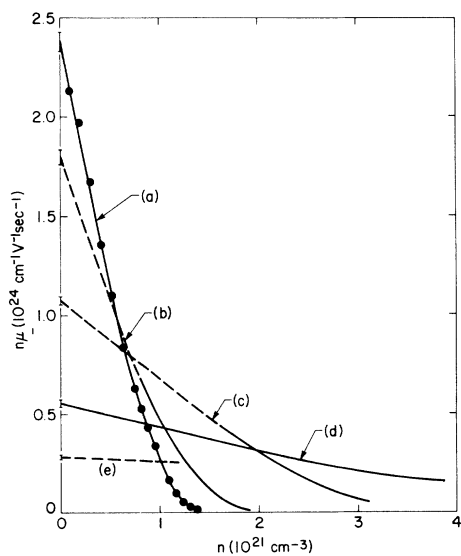


FIG. 9. $n\mu$ as a function of n at various temperatures: curve (a) 4.2 K, this work; curve (b) 7.3 K, Ref. 10; curve (c) 20.3 K, Ref. 11; curve (d) 77.6 K, Ref. 6; curve (e) 293.2 K, Ref. 5. Dashed lines indicate where best-guess corrections for electron-heating effects have been made.

tic electron wavelength λ_T becomes significant compared with the mean-free path l , then one is tempted to try to fit the initial deviation from μ_{class} by $\mu \approx \mu_{\text{class}}(1 - \alpha\lambda_T/l)$. This becomes

$$\mu \approx \mu_{\text{class}}(1 - cnT^{-1/2}) \quad (2)$$

with $c = h\sigma\alpha(2\pi mk)^{-1/2}$ when the usual expressions $\lambda_T = h(2\pi mkT)^{-1/2}$ and $l = (n\sigma)^{-1}$ are substituted. In addition to predicting the linear decrease of $n\mu$ with increasing n , Eq. (2) also gives the approximate temperature dependence of the rate of decrease. As shown in Fig. 10, the normalized slope is indeed closely proportional to $T^{-1/2}$, with a value of c which corresponds to $\alpha \approx \frac{1}{2}$. There is some evidence of an upward curvature in the data points of Fig. 10, and this may arise from correlations in the positions of the scatterers. To first order, correlations give rise to a modified mobility⁹

$$\mu = \mu_{\text{class}}[1 + 2nB(T)], \quad (3)$$

where $B(T)$ is the virial coefficient of the gas. Thus, one should add a term $-2B(T)$ to the normalized slope, a correction which is of the right order to account for the observed deviation from a strict $T^{-1/2}$ dependence. Although the argument that led us to Eq. (2) cannot be taken seriously, its success suggests that a rigorous derivation may be possible.

Figure 7 gives the mobilities in the region where they are dropping rapidly. The results are in essential agreement with the original observations of Levine and Sanders, but relatively small temperature differences are now well resolved and

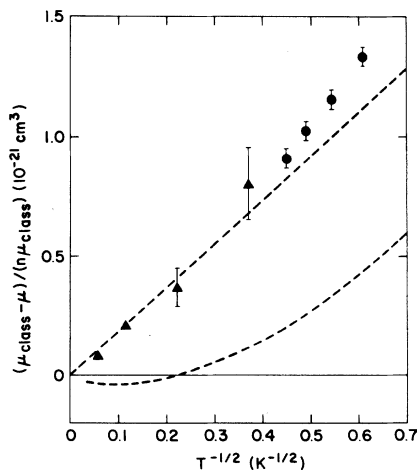


FIG. 10. Normalized slopes of the initial linear deviations from μ_{class} . Circles are our data, triangles are from Refs. 5, 6, and 10. The upper curve shows the prediction of Eq. (2) where α equals $\frac{1}{2}$. The lower curve shows the correction $-2B(T)$ which should be added to the upper curve to account for correlations.

significant new information about the shape of the drop-off curves is obtained. A synthesis of the electron-localization curves is shown in Fig. 11, which combines our data with the higher-temperature results of Refs. 6 and 10. This figure presents the systematics of the transition in the striking fashion, showing how the electrons localize as their thermal energy is reduced, and how the classical Boltzmann limit is approached at high temperatures or low densities. Interpretation of these curves, in conjunction with those of Figs. 6 and 9, presents the main theoretical challenge.

A somewhat extraneous point needs to be made here. As has been mentioned before, the historical tendency has been to treat the initial drop-off (Fig. 1) and the localization (Fig. 2) as distinct phenomena. This has perhaps been reinforced by the fact that when plotted as in Fig. 2, the mobility curves appear to show a break in slope at $n \approx 1.0 \times 10^{21} \text{ cm}^{-3}$, in agreement with the prejudice that the localized states are not formed until a critical density of this magnitude is reached. It is, however, obvious from Fig. 12 that the break in slope is an artifact of the way in which the data have historically been plotted, and that it would be present for any $\mu(n)$ which decreases more or less uniformly with increasing n . Thus, the experimental results do not in themselves imply that two different mechanisms need to be considered.

At still higher densities (or lower temperatures) μ approaches a slowly-varying limiting behavior which is reminiscent of the propagation of heavy impurity ions. This regime has been analyzed by assuming that the nature of the localized states available to the electron are such that its wave function occupies a spherical region of radius R . If one assumes that such a localized state moves through the gas as if it were a solid sphere, one

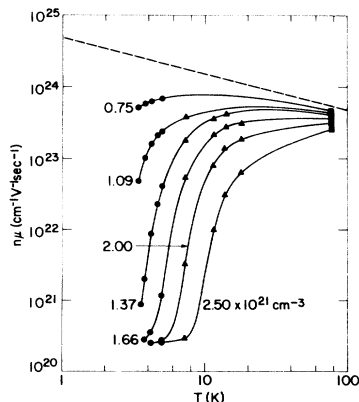


FIG. 11. Constant-density electron-localization curves. Circles represent our data, triangles the data of Ref. 10, and squares the data of Ref. 6.

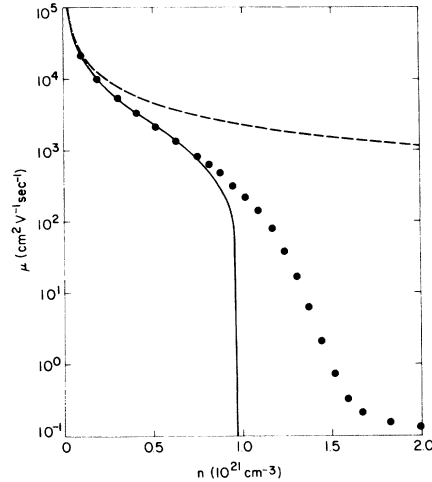


FIG. 12. 4.2-K values of μ , plotted in the manner of Refs. 9–11. The dashed curve is the classical mobility, the solid curve is a straight-line fit to the low-density values, as in Fig. 6.

can use the interpolation formula⁹

$$\mu = \frac{e}{6\pi\eta R} \left(1 + \frac{9\pi\eta}{4nR(2\pi m_4 kT)^{1/2}} \right), \quad (4)$$

where η is the gas viscosity, and m_4 is the mass of a helium atom. As shown in Fig. 8, Eq. (4), with $R \approx 16 \text{ \AA}$, gives a very good fit to the observed mobility. The fitted value $R \approx 16 \text{ \AA}$ is in reasonable agreement with the expected radius of the localized wave function as deduced from variational calculations,^{9,10} and there appears to be little doubt that in this regime the electron is permanently trapped in a deep “bubble” state.

B. Nonlinear behavior

In the region where μ is strongly depressed by localization effects, the drift velocity curves exhibit rather spectacular nonlinearities (Fig. 13).

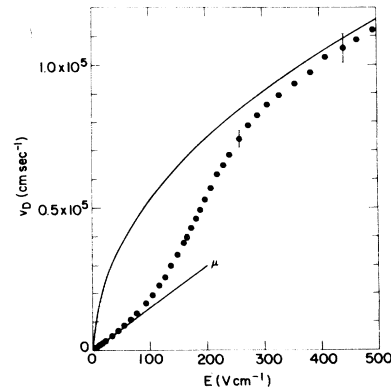


FIG. 13. Typical $v_D(E)$ curve. The points are experimental results (with representative errors as shown) taken at $T = 4.20 \text{ K}$, $n = 1.089 \times 10^{21} \text{ cm}^{-3}$. The upper curve is the classical $v_D(E)$.

One can argue qualitatively that, as the electrons heat up, they spend less time in the low-lying localized states and thus tend to approach the classical limit. The details of how this occurs are of obvious interest as providing an additional test of any model for the zero-field mobilities described previously. It is therefore somewhat surprising that, except for the original observations of Levine and Sanders and the high-temperature studies of Bartels, no significant information about the nonlinear behavior has been obtained.

Figure 14 shows how $v_D(E)$ varies with density at 4.20 K. These curves exhibit a number of interesting features. As has already been discussed, there is a rapid drop in the mobility as n increases. In this region, electron-heating effects manifest themselves as a supralinear deviation tending to approach the classical hot-electron limit. The drift velocity at which nonlinearity is first observed drops sharply with increasing n , reaching values below 100 cm sec^{-1} . As the electrons become fully localized, however, this velocity increases again.

Sets of curves such as in Fig. 14 were also obtained at other temperatures. A direct comparison of these data with Fig. 14 is not particularly il-

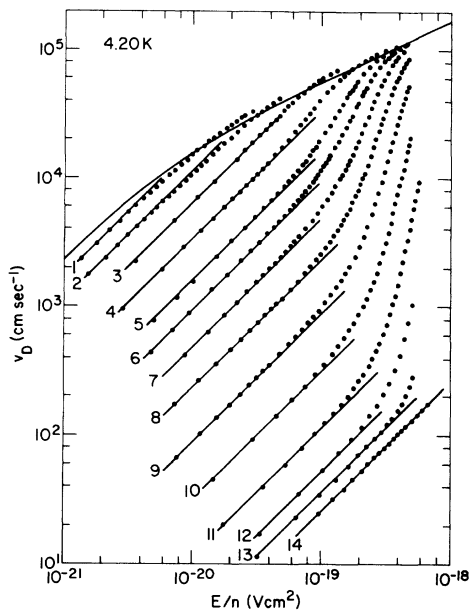


FIG. 14. Density dependence of $v_D(E)$ at 4.20 K. The densities for the various curves are (in units of 10^{21} cm^{-3}): 1—0.301; 2—0.518; 3—0.749; 4—0.948; 5—1.089; 6—1.165; 7—1.236; 8—1.304; 9—1.373; 10—1.441; 11—1.513; 12—1.587; 13—1.663; 14—1.824. The straight lines drawn through the data points indicate the linear response at low fields. The upper curve is the classical result computed from the Druvsteyn equation using $\sigma(E)$ as given in Ref. 2.

luminating since they are qualitatively very similar. Instead, we show in Figs. 15–17 the variation of $v_D(E)$ with temperature for various fixed values of n . In order to facilitate comparison with the density variation, the results are plotted on a grid of curves obtained by smoothing the 4.20-K data. It is particularly striking that a decrease in T with n fixed has nearly the same effect on the shape of these curves as an increase in n with T fixed. Upon closer examination, however, there is evidence that as T increases the nonlinear part of $v_D(E)$ becomes relatively less steep. This is qualitatively consistent with the fact that the 76.8-K measurements of $v_D(E)$ do not exhibit a pronounced supralinear behavior.

One peculiar feature of Figs. 14–17 which, although minor compared with the drastic variations arising from localization, is still outside of the error estimates is that $v_D(E)$ appears to overshoot slightly the classical drift velocity at high fields and then to return to the classical limit at still higher fields. Bartels⁶ sees no such effect at 76.8 K, while the 4.20-K measurements of Levine and Sanders are not sufficiently accurate to tell. It was initially assumed that this overshoot represented some kind of systematic error in the measurements. However, the effect resisted all efforts at elimination and must be tentatively regarded as real.

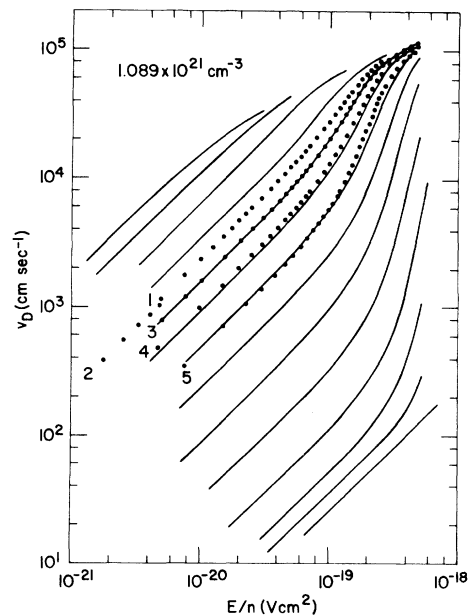


FIG. 15. Temperature dependence of $v_D(E)$ for $n = 1.089 \times 10^{21} \text{ cm}^{-3}$. The temperatures for the various sets of data are 1—4.98 K, 2—4.60 K, 3—4.20 K, 4—3.80 K, 5—3.40 K. The solid curves are smoothed fits to the data of Fig. 14.

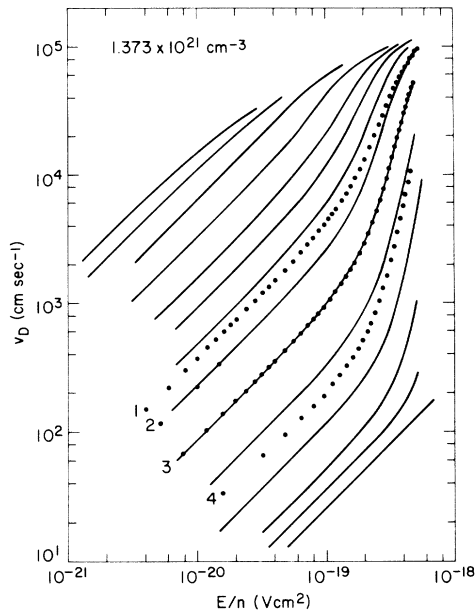


FIG. 16. Temperature dependence of $v_D(E)$ for $n = 1.373 \times 10^{21} \text{ cm}^{-3}$. The temperatures for the various sets of data are 1—4.98 K, 2—4.60 K, 3—4.20 K, 4—3.80 K. The solid curves are smoothed fits to the data of Fig. 14.

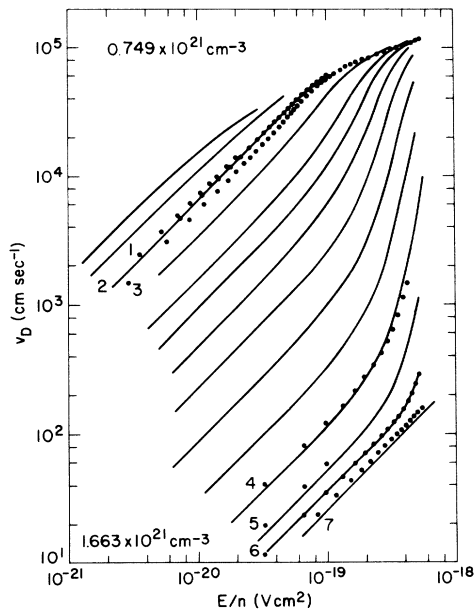


FIG. 17. Temperature-dependence of $v_D(E)$ for $n = 0.749 \times 10^{21} \text{ cm}^{-3}$ and $1.663 \times 10^{21} \text{ cm}^{-3}$. The temperatures for the various sets of data are 1—4.98 K, 2—4.20 K, 3—3.40 K, 4—4.98 K, 5—4.60 K, 6—4.20 K, 7—3.80 K. The solid curves are smoothed fits to the data of Fig. 14.

To close this section, we note that even at the shortest drift times ($\sim 10 \mu\text{sec}$) no evidence for pulse broadening was observed. Thus, the time required by a given electron to take an average over the accessible states is much shorter than this flight time. Young²¹ has suggested that the supralinear $v_D(E)$ seen experimentally arises because the electrons start out in extended states and decay into localized states in some characteristic times comparable to the flight time. A later paper by the present author,²² in which the transmission characteristics of a chopper grid were used in an attempt to separate fast and slow electrons appeared to lend support to this hypothesis. The present work, however, shows that such an interpretation is erroneous.²³

IV. DISCUSSION

This section is not intended as a complete catalog of previous attempts at dealing theoretically with various aspects of the problem, nor does it present any new efforts along these lines. The aim is more to assess the success and current status of theoretical models in which the helium-gas-plus-electron system is treated as a solid-state type of random potential problem.

As discussed in Sec. I, the actual potential experienced by the electron closely resembles a gas of randomly placed hard spheres. The gas is at once dilute, in the sense that $na_0^3 \ll 1$, and dense, in the sense that only electron wave functions which overlap many scattering centers will turn out to be of interest. Although attempts have been made to attack this problem from first principles using cluster expansion techniques,²⁴ this approach has so far proved too difficult to yield any insight into the localization process, or indeed to yield predictions which agree with experiment. Further progress along these lines may, however, be possible.²⁵ The more usual expedient is to separate the problem into two parts, first computing the average effect of the potential by treating the multiple scattering from the hard cores in some approximation, and then worrying about how fluctuations in the average properties, arising from statistical variations in the local density of scatterers, give rise to localized states.

A. The Egarter-Cohen model

The most comprehensive treatment of this type is the quasiclassical percolation model of Egarter and Cohen.^{14,26} The authors use a Wigner-Seitz argument to estimate the average potential $V(n)$, thus taking approximate account of the effect of higher-order multiple scattering corrections to the electron energy. They then divide the system

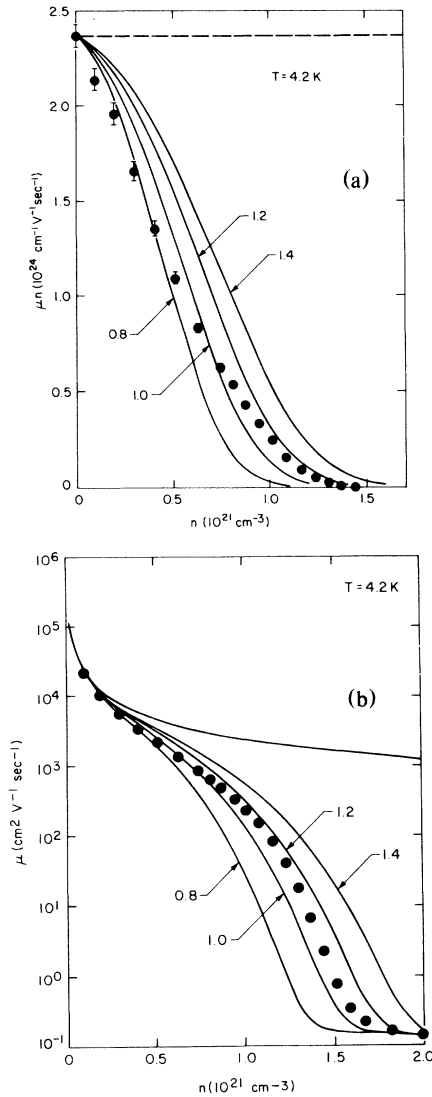


FIG. 18. (a) Predictions of the modified Eggarter-Cohen model (solid curves) for various values of c , with emphasis on the initial drop-off. (b) Predictions of the modified Eggarter-Cohen model with emphasis on the localization behavior.

into boxes of volume $L^3 = (c\lambda)^3$ to determine a fluctuating local density $n(\vec{r})$ and potential $\bar{V}(\vec{r})$, in a manner similar to that discussed in Sec. I. Here λ is the free-space wavelength of the electron and c is a parameter adjusted to fit the experimental results. The authors make no serious attempt to calculate the electron states in this potential, but instead use quasiclassical counting²⁷ to determine the density of states. The degree of localization of the states at a given energy is deduced from classical percolation theory,²⁸ and an average

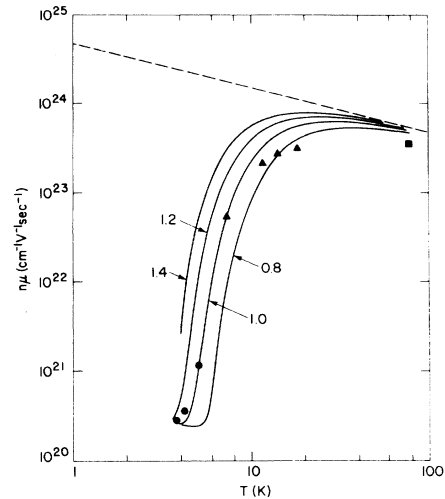


FIG. 19. Predicted temperature-dependent mobility, for various values of c . The calculations and the data points correspond to $n = 1.66 \times 10^{21}$.

classical mobility is assigned to each extended state. The resulting theory, although quite phenomenological, has the virtue of making specific predictions which can be compared with experiment.

Figures 18(a) and 18(b) show $\mu(n)$ at 4.20 K as predicted by the Eggarter-Cohen model, while Fig. 19 shows $\mu(T)$ at $n = 1.66 \times 10^{21}$. As has been found in previous numerical work,^{14,29} the model gives a surprisingly good account of itself when compared to the data as in Figs. 18(b) and 19.³⁰ The most interesting new insight to arise from the present calculations is that the Eggarter-Cohen model also predicts the roughly linear initial drop-off in μn as n increases [Fig. 18(a)]. It is not clear exactly how this result relates to the recent theory of Braglia and Dallacasa,³¹ in which the initial drop-off is explained on the basis of certain assumptions about the single-scatterer t matrix, or indeed to other, previous attempts³²⁻³⁴ to explain the drop-off on the basis of multiple-scattering theory. Nevertheless, all successful efforts of this type^{14,31,34} share the feature that states below the average potential are assumed to have a very small mobility. It is this feature, and not some modification in the transport properties of the extended states, which appears to give rise to the initial drop-off.

The Eggarter-Cohen model, while it is simple, intuitively appealing, and rather successful, is also quite phenomenological and somewhat controversial. Many features of this model can be justified from a variational point of view,³⁵ but further

progress would seem to require a more detailed theoretical treatment. In the remainder of this paper we discuss how the helium gas problem can be related to current approaches in the theory of disordered systems.

B. Other models

In the Eggarter-Cohen theory, the choice of the averaging scale L strongly affects the predicted behavior: Certain unclear assumptions about the nature of the wave functions are implicit in this choice, as well as in the way that the density of states $N(\epsilon)$ is evaluated. To take a more fundamental approach, one can begin by averaging the individual scatterers over some small volume a^3 , where we use a different notation to emphasize the fact that this fine-scale smoothing of the potential is now to be interpreted as a mathematical artifice. Thus, a is arbitrary, except that it should be large enough to generate a Gaussian distribution of the local density $\tilde{n}(\vec{r})$ and hence $\tilde{V}(\vec{r}) = V[n(\vec{r})]$. For $V(n)$ one can use either the "optical potential" $V(n) = 2\pi\hbar^2 a_0 n/m$, or the more realistic Wigner-Seitz estimate of Eggarter and Cohen. In either case, one ends up with a Gaussian distribution $\tilde{V}(\vec{r})$, which has an autocorrelation function $\langle \tilde{V}(\vec{r})\tilde{V}(\vec{r}') \rangle$ with a range of order a .

The object now is to find the density of states and the (pseudo) wave functions belonging to this potential, without resorting to quasiclassical arguments. For energies such that the wave functions do not change appreciably over distances of order a , $\langle \tilde{V}(\vec{r})\tilde{V}(\vec{r}') \rangle$ acts essentially as a δ function, and one may expect that the results will in some sense become independent of the choice of a . The physical idea is that the overall properties of wave functions which extend over many scatterers are not affected by minor rearrangements in the positions of the scatterers, and hence should be insensitive to a fine-scaled smoothing of the potential. It appears that this "white noise" limit is indeed a reasonable approximation in the case of the helium-gas problem, at least near the mobility edge. Other systems to which this description is thought to be relevant are semiconductors containing a high density of impurities,³⁶ and metal-oxide semiconductor inversion layers.³⁷

The problem of the Gaussian random potential in more than one dimension has by no means been solved, even in the white noise limit. Several very illuminating papers³⁶⁻³⁹ have dealt with the problem of counting states for energies far below the mobility edge, where the electron states occur because of deep, highly localized, and widely separated downward fluctuations of $\tilde{V}(\vec{r})$. Halperin⁴⁰ has shown that the calculation of deep-lying fluctuation

states is in fact a sophisticated version of the bubble-transition calculations which have traditionally been applied to the problem of electron localization in helium gas.^{9,10,41} The fluctuation theory approach is more refined in that it treats correctly the translational degrees of freedom of the localized states, and in that it shows how the approximations involved in the traditional bubble calculations break down as ϵ approaches the mobility edge. Simply put, as ϵ increases, the available states become more numerous and more extended: at some point, they will begin to mix strongly, and the picture of isolated bubble-type states becomes inappropriate.⁴² There is no good theory for $N(\epsilon)$ in this regime. One may remark that the traditional bubble calculations, which ignore all of these complications and simply compare the free energies of extended and localized states, may correctly estimate the approximate values of n and T for which the localized states become highly favorable, but they cannot be expected to yield a correct description of the transition behavior.

The preceding discussion indicates that it is a matter of current interest to develop a theory which matches the deeply localized fluctuation states to a reasonable model for $N(\epsilon)$ at higher energies. The helium-gas system appears likely to provide a suitable test case for such models. We conclude by pointing out that there are two theoretical approaches which at the moment seem particularly promising. The first of these is to examine the manner in which the Halperin-Lax theory breaks down, in order to make a connection with the percolation model of Eggarter and Cohen. When the localized states $\psi_0(\epsilon)$ become sufficiently large and numerous to mix strongly, one presumably goes over to a regime featuring irregularly shaped, extended, shallow potential wells occupied by electron states closely spaced in energy. This is the qualitative picture assumed by Eggarter and Cohen, where one can now identify their smoothing parameter L as the characteristic radius of $\psi_0(\epsilon)$ at that value of ϵ where mixing becomes important. Thus one may be able to justify some of the *ad hoc* features of the percolation model.

A second interesting possibility is to adapt the recent work of Thouless and Elzain³⁷ on localization in inversion layers to the helium-gas problem. These authors generate a tight binding version of the white noise problem, again by averaging the potential over small volumes of size a^3 . This allows them to apply the coherent potential approximation (CPA) formalism to the extended states in a regime where it is expected to work well. By interpolating between the deep fluctuation state regime and the CPA regime, Thouless and Elzain

obtain a description which is in good agreement with their numerical simulations of the two-dimensional white noise problem. There appears to be no reason why this approach could not be extended to the three-dimensional case, with a view toward trying to fit the helium-gas results.

ACKNOWLEDGMENTS

The author wishes to thank J. R. Barker, M. H. Cohen, J. P. Hernandez, S. Kirkpatrick, and D. J. Thouless for helpful discussions.

- ¹T. F. O'Malley, *Phys. Rev.* **130**, 1020 (1963).
²R. W. Crompton, M. T. Elford, and A. G. Robertson, *Aust. J. Phys.* **23**, 667 (1970).
³Since only *s*-wave scattering is important here, the momentum transfer cross section $\int (1 - \cos\theta)\sigma(\theta)d\omega$ is equal to the total scattering cross section.
⁴This equation is valid only to the extent that $\sigma(kT) = \sigma_0$.
⁵R. Grünberg, *Z. Naturforsch.* **24a**, 1838 (1969).
⁶A. Bartels, *Appl. Phys.* **8**, 59 (1975).
⁷J. J. Lowke, *Aust. J. Phys.* **16**, 115 (1963).
⁸R. Grünberg, *Z. Naturforsch.* **23a**, 12 (1968).
⁹J. L. Levine and T. M. Sanders, Jr., *Phys. Rev.* **154**, 138 (1967); J. L. Levine, Ph.D. thesis, University of Michigan, 1965 (unpublished).
¹⁰H. R. Harrison, L. M. Sander, and B. E. Springett, *J. Phys. B* **6**, 908 (1973); H. R. Harrison, Ph.D. thesis, University of Michigan, 1971 (unpublished).
¹¹J. A. Jahnke, M. Silver, and J. P. Hernandez, *Phys. Rev. B* **12**, 3420 (1975).
¹²L. L. Foldy, *Phys. Rev.* **67**, 107 (1945).
¹³M. Lax, *Rev. Mod. Phys.* **23**, 287 (1951).
¹⁴T. P. Eggarter, *Phys. Rev. A* **5**, 2496 (1972).
¹⁵K. W. Schwarz, *Phys. Rev. Lett.* **41**, 239 (1978).
¹⁶K. W. Schwarz, *Phys. Rev. A* **6**, 837 (1972).
¹⁷J. E. Kilpatrick, W. E. Keller, and E. F. Hammel, *Phys. Rev.* **97**, 9 (1955).
¹⁸W. E. Keller, *Phys. Rev.* **97**, 1 (1955).
¹⁹P. R. Roach, *Phys. Rev.* **170**, 213 (1968).
²⁰O. B. Verbeke, *J. Res. Natl. Bur. Stand.* **76A**, 207 (1972).
²¹R. A. Young, *Phys. Rev. A* **2**, 1983 (1970).
²²K. W. Schwarz and B. Prasad, *Phys. Rev. Lett.* **36**, 878 (1976).
²³Computer simulations show that the effects reported in Ref. 22 can be interpreted as arising from the sharp nonlinearities in $v_D(E)$ as shown in Fig. 14.
²⁴H. E. Neustadter and M. H. Coopersmith, *Phys. Rev. Lett.* **23**, 585 (1969); M. H. Coopersmith, *Phys. Rev. A* **4**, 295 (1971).
²⁵J. R. Barker (private communication).
²⁶T. P. Eggarter and M. H. Cohen, *Phys. Rev. Lett.* **25**, 807 (1970); **27**, 129 (1971).
²⁷E. O. Kane, *Phys. Rev.* **131**, 79 (1963).
²⁸See, for example, S. Kirkpatrick, *Rev. Mod. Phys.* **45**, 574 (1973).
²⁹J. P. Hernandez, *Phys. Rev. A* **5**, 635 (1972).
³⁰The extremely good agreement found in some of the earlier calculations appears to be fortuitous.
³¹G. L. Braglia and V. Dallacasa, *Phys. Rev. A* **18**, 711 (1978).
³²W. Legler, *Phys. Lett. A* **31**, 129 (1970).
³³I. T. Yakubov, *Zh. Eksp. Teor. Fiz.* **57**, 1040 (1969) [*Sov. Phys. - JETP* **30**, 567 (1970)]; V. M. Atrazhev and I. T. Yakubov, *J. Phys. D* **10**, 2155 (1977).
³⁴T. F. O'Malley (unpublished).
³⁵P. Lloyd and R. Best, *J. Phys. C* **8**, 3752 (1975).
³⁶B. I. Halperin and M. Lax, *Phys. Rev.* **148**, 722 (1966).
³⁷D. J. Thouless and M. E. Elzain, *J. Phys. C* **11**, 3425 (1978).
³⁸B. I. Halperin and M. Lax, *Phys. Rev.* **153**, 802 (1967).
³⁹J. Zittartz and J. S. Langer, *Phys. Rev.* **148**, 741 (1966).
⁴⁰B. I. Halperin, *Phys. Fenn.* **8**, 215 (1973). We wish to emphasize a point, mentioned in passing in Halperin's paper, which often causes confusion and does not appear to be generally appreciated. Because an injected electron will cause a hole to develop in the gas when it goes into a bubble state, it at first sight seems that the free-energy arguments, which concentrate on the states occupied by a particular electron, are talking about something different from the fluctuation calculations, where naturally occurring density fluctuations in an infinite medium are enumerated. The definition of the free energy, however, involves an equivalent state counting procedure, provided that the electron energy can be well defined. The distinction drawn by our intuition applies to the dynamics of how fast the electron gets from one state to another, not to the relative probability of occupation.
⁴¹J. P. Hernandez, *Phys. Rev. B* **11**, 1289 (1975).
⁴²A very qualitative form of this argument has been advanced by T. P. Eggarter and M. H. Cohen, *J. Phys. C* **7**, L103 (1974) in defense of their semiclassical model against a criticism advanced by J. P. Hernandez and J. M. Ziman, *J. Phys. C* **6**, L251 (1973).